International Journal of Science and Research (IJSR)
ISSN (Online): 2319-7064
Index Copernicus Value (2013): 6. 14 | Impact Factor (2013): 4. 438

Characterization of Nanorods Obtained by Mixing 20%SnO_2 + 80% In_2O_3 Thin Films Prepared by Sol-Gel Method

Melia Hamici[1], Adel Hachache[2]

[1]Setif 1 University, DAC laboratory, 19000 Algeria
[2]Nîmes University, MIPA Laboratory 30000, France

Abstract: ***In this work a mixing $SnO_2$and In_2O_3 precursors solutions were prepared by sol-gel method. About this mixture, thin films were elaborated by dip coating and were followed by annealing in air. Nanorods were obtained and were appeared for 20% SnO_2+ 80% In_2O_3 of mixture. The morphology composition and structure layers were studies by scanning electron microscopy and X ray diffraction. The optical transmission of these films is in the order of (up to 95%), with a band gap of 3. 27eV. The best film showed a significant decrease of its square resistance $R_{\square}$ (down to12 Ω/□). This result is an excellent value obtained by sol-gel method.***

Keywords: In_2O_3, SnO_2, thins films, square resistance, morphological properties, XRD analysis, AFM images

1. Introduction

As an important Transparent conducting oxides (TCO), Indium oxide (In_2O_3) and SnO_2 were attracted considerable attention due to their special optical and electrical properties. Indium oxide (In_2O_3) has attracted considerable attention because of its high electron affinity and increasingly extensive application in solar cells [1]-[4], sensors [5], nanoscole transistors [6], and flat –panel display materials [7]. More recently, there has been considerable attention on the synthesis of In_2O_3 nanostructures in order to endow nanomaterials with additional properties or potential application [8]. On the other hand, tin oxide (SnO_2) as a n-type semiconductor, have a variety of application as optical filters, heat deflectors, high–stability resistors, covering layers for fiber optical systems, switches, detecting elements of ecological monitoring sensors measuring the concentration of toxic [9] and explosive gases[10]-[13], transparent electrodes [14]-[15].

To grow In_2O_3 and SnO_2 thins films several techniques have been used such as cathode sputtering [16]-[17], canon ray evaporation [18], Pulverization with subsequent pyrolysis [19], laser pulse evaporation [20]-[21] and sol-gel deposition [22]-[23].

In the present work, we report the synthesis and characterization of films obtained by mixture of two solutions of In_2O_3 and SnO_2.

2. Experimental

(100-x)% SnO_2+ x %In_2O_3 precursors mixture was prepared using sol-gel method where x is 0, 20, 40 and 80 of mixture. SnO_2 was prepared by dissolving 3.4g of tin chloride dihexahydrate ($SnCl_2$, $2H_2O$) in 42.5 ml of ethanol and 7. 5ml of acetic acid. The solution was stirred at 60 C° for 2h to yield a clear yellow and homogeneous solution, the solution was stored 72h before used. In_2O_3, was prepared by dissolving 1.59g indium chloride ($InCl_3$) in 18 ml of acetyl acetone ($CH_3CH_2COCH_3$), the solution was stirred at 80°C for 12h to yield a clear brown solution.

Both solutions were mixed with different percentage of In_2O_3 ranging from 0%, to 80%, under magnetically stirring for 10 min at room temperature to obtain a homogenous sol; a glass substrate was dipped in the solution. The deposited films were dried at 150°C for 10min.

The dip coating and drying processes were repeated twice to deposit relatively thick thin films. Finally, the annealing temperature was elevated to 500°C for 1 hour.

Surface morphology of prepared thin films was investigated using scanning electron microscopy (SEM) (JEOL JSM 7001F field emission) and Atomic force microscopy (AFM) (PACIFIC NANOTECHNOLOGY). X ray diffraction (XRD) (BRUKER – AXS D8) spectrum was recorded to examine the crystal structure.

The optical property was examined by UV-VIS spectrometer (Hitach V3000). The index factor was determined by fitting method [24].

3. Results and Discussions

The XRD patterns of synthesized SnO_2-In_2O_3 thin films calcined at 500°C for 1h are showing in Fig. 1. The XRD patterns of all samples shows the dominant peaks which represent the indices of (110) and (101) planes, respectively, correspond to rutile SnO2 phase (ASTM file *N*° : 6-416). The average crystallite size was found to be 83. 37nm. Moreover, it can be observed that the peak intensities progressively decrease with increasing In_2O_3 precursor percentage, possibly indicating that an increase in the In_2O_3 percentage retards the crystallization process of the SnO_2 [25]. When the SnO_2 oxide was mixing with 40% and 80% of In_2O_3 percentage, the two phases appear (Fig. 1c and Fig. 1d, the first one with peaks appearing to indices of (222), (200) and (211) planes corresponding to the cubic In_2O_3 phase (JCPDS

Licensed Under Creative Commons Attribution CC BY

Card N° 06-0416) [26], and the second of rutile SnO_2; these results indicate that the incorporation of In_2O_3 precursor percentage delay rutile SnO_2 phase formation. For 80% of In_2O_3, a separation of the In_2O_3 phase was observed with average crystallite size about 83. 98nm. This implies that as long as the In_2O_3 phase is preserved and is significantly separated from the SnO_2-In_2O_3 mixed oxides phase, therefore an excess of In_2O_3 Inside the matrix of the rutile SnO_2 phase.

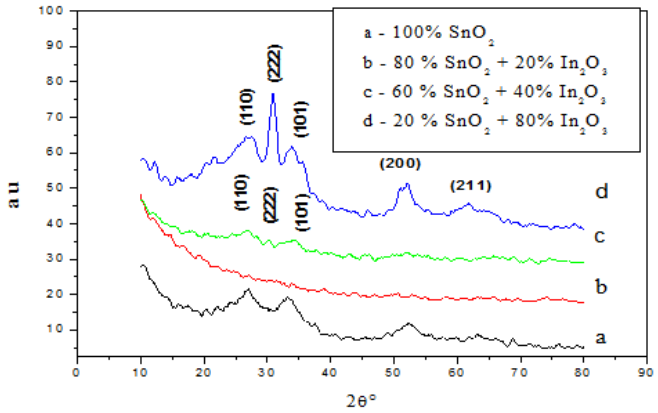
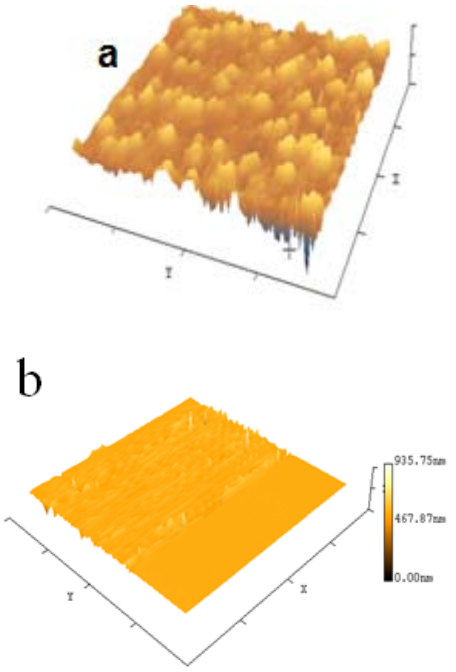


Figure 1: XRD pattern of (a) pure SnO_2, (b) 80%SnO_2+20% In_2O_3, (c) 60%SnO_2+40% In_2O_3 and (d) 20%SnO_2+80% In_2O_3 films annealed at 500°C

Fig. 2 shows the topography of the SnO_2- In_2O_3 thin films deposited at room temperature, with different In_2O_3 precursor percentage. Fig. 2a shows granular microstructure containing regular spherical particles of SnO_2, the roughness parameter Rms is respectively 20.79 nm. Fig. 2b shows an amorphous structure; Fig. 2. c shows image of 60% SnO_2 + 40%In_2O_3 film. We note the coexistence of two morphologies with different particles sizes smaller one and the biggest one, the morphology changes significantly with the Indium oxide percentage.



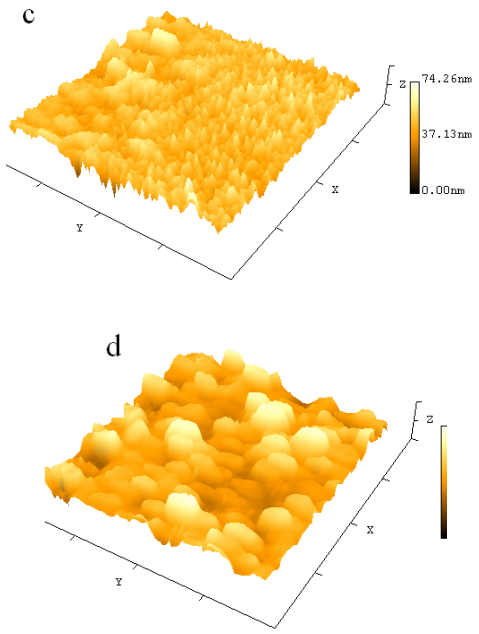


Figure 2: AFM images of (a) pure SnO_2, (b) 80% SnO_2+ 20% In_2O_3, (c) 60% SnO_2 + 40%In_2O_3 and (d) 20% SnO_2 +80% In_2O_3 thin films

Fig. 2d shows irregular spherical particles corresponding to 20%SnO_2+80% In_2O_3 film, it is rougher and has a large active surface area, with roughness parameter Rms 37, 46 nm. The average roughness increases with increasing the In_2O_3 precursor percentage. In the same way, it has been reported that the grain size enlargement is related with the increase of the film thickness [27].

The SEM images of the synthesized SnO_2-In_2O_3mixed precursors oxides is exemplified in Fig. 3. The SEM image shows the quite uniform-size particles of the pure SnO2 Fig. 3A in the form of aggregated clusters consisting of many nanoparticles. Fig. 3B shows an amorphous structure without particle. When considering the 20%SnO_2+80%In_2O_3 mixed oxide it can be clearly seen that higher percentage of In_2O_3 led to nanorods formation with 200 nm length and 20nm width without direction and with randomly oriented as expected.

Fig. 3C and Fig. 3D, shows morphology surface at θ=35 °. Once again we can conclude that the particle shape is strongly affected by In_2O_3 mixture percentage.

Licensed Under Creative Commons Attribution CC BY

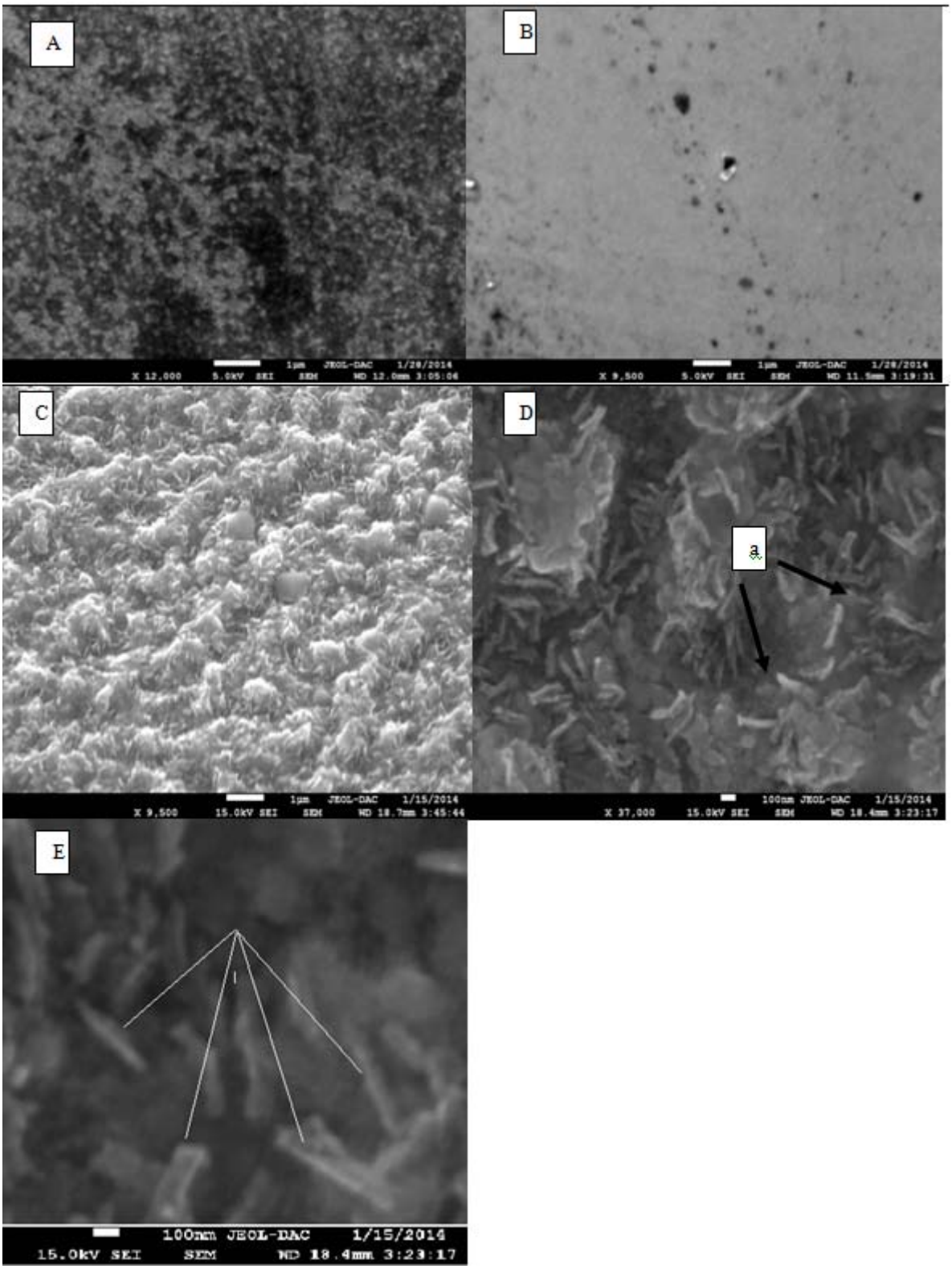


Figure 3: SEM images of SnO_2-In_2O_3 mixture, (A) pure SnO2, (B) 80%SnO_2+20%In_2O_3, (C) 20%SnO_2 + 80% In_2O_3 (X9500), (D) and (E) Nanorods.

4. Electrical Properties

Fig. 4 shows Electrical properties measurement was done by four probe method, In order to determine square resistance *R* (Ω/□) of SnO_2-In_2O_3 thin films. Square resistance R (Ω/□) of the pure SnO_2 films, gives immediately 538.42 (Ω/□). By addition of 40 % In_2O_3 ratio to SnO_2 leads to significant resistance drop about 284 (Ω/□). With 80% of In_2O_3, specific resistance decrease in about 9-10 orders of magnitude, reaching 11.73 (Ω/□). This low value is strongly performed by increasing the number of charge carriers (electrons) from donors In^{3+} ions incorporated in the interstitial or substitutional sites of Sn^{+2} cation and the presence of nanorods (confirmed by SEM).

Licensed Under Creative Commons Attribution CC BY

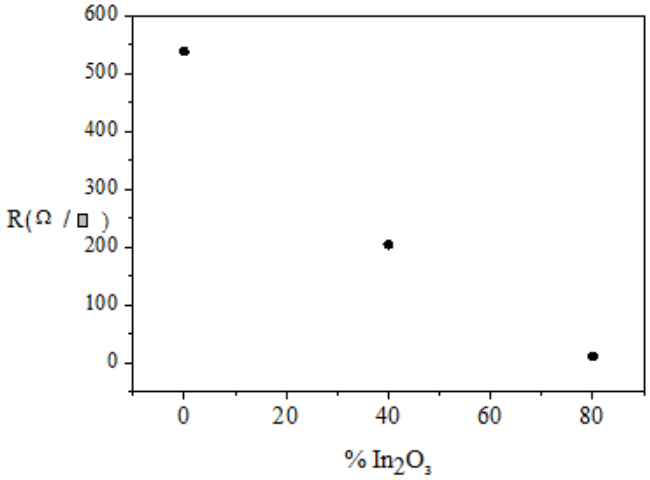
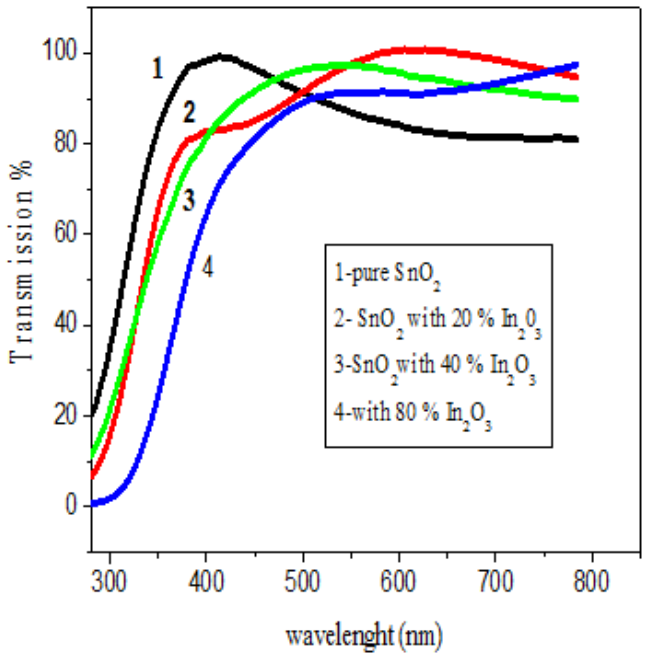


Figure 4: Square resistance of thin films for different % of In_2O_3

5. Optical Properties

Fig. 5 shows the Uv-Vis transmission spectra of SnO_2-In_2O_3 thin films the films annealed at 500°C for 1 h, with 0%, 20 %, 40% and 80% In_2O_3 mixture exhibit a transmission of 95% in the visible region for all films. It is found that transmission increases with increasing concentration of In_2O_3 mixture, amorphous film obtained for a mixture of 20% In_2O_3, presents a most transmission and thus exceeds the transmission of pure SnO_2.



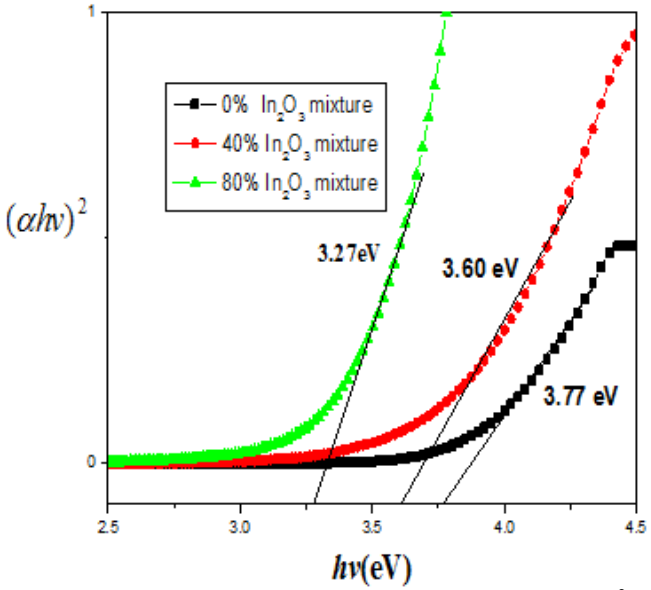


Figure 5: (a) Optical transmission and (b) curve $(\alpha h\nu)^2$ versus (hv) at different percentage of In_2O_3

Band gap (*Eg*) of these films has been calculated from transmission spectra using Tauc's formula [28]:

$$\alpha h\nu = A(h\nu - E_g)^{1/2} \quad (1)$$

In which α is the absorption coefficient, *hv* is the photon energy, and A is constant related to the material. Plot of $(\alpha h\nu)^2$ vs (*hv*) for SnO_2 -In_2O_3 thin films Fig. 5b. It is found that (E_g) decreases with changing the mixture of In_2O_3. The estimated optical band gap for the pure SnO_2, 40% and 80% of films are found to be 3. 77eV, 3. 6eV and 3. 27eV respectively, which could be assigned due to change in the grains shape or (and) size. The refractive index *n* and the films thickness *t* are fitted according to Sellmeier relationship [24], given by:

$$n(\lambda) = \left(A_n + \frac{B_n\lambda^2}{\lambda^2 - C_n^2}\right)^{-\frac{1}{2}} \quad (2)$$

Where A_n, B_n and C_n are fitting parameters. The refractive index *n* was found to be 2.26,1. 45, 1.75, and 2.01 for the 0%, 20%, 40% and 80% of In_2O_3 percentage respectively, the value of the refractive index of SnO_2 seems to be in good agreement with earlier results of [29].

6. Conclusion

In this paper, ITO thin films were elaborated by sol-gel Dip-Coating process. XRD spectra indicate that pure SnO_2 is formed with rutile structure. It is found that addition of 80% Indium-oxide modify the structure of tin-oxide from nanoparticules to nanorods, those nanorods are without orientation. It was found that varying Indium-oxide concentration strongly affects electrical properties, square resistance achieved a value 11.73 (Ω/□), this value has never been obtained by sol gel method. The Uv-Vis spectra show that transmission is about 95% in the visible region for all films.

Licensed Under Creative Commons Attribution CC BY

References

[1] J. Parendo, R. Santhanam, F. Mijangos, B. Rambabu, Int. J. Electrochem, pp. 1342-1354, 2010.
[2] A. O. Neto, R. W. R. Vergilio-Silva, M. Linardi, E. V. Spinace, Int. J. Electrochem, pp 954-961, 2009.
[3] J. A. run Kumer, P. Kalyani, R. Saravanan, int. J. Electrochem, pp 961-969, 2008.
[4] B. Krishnamurthy, S. Deepalochani, J. Electrochem, pp 386-395, 2009.
[5] D. Zhang, Z. Liu, C. Li, T. Tang, X. Liu, S. Han, B. Lei, C. Zhou, Nano Lett, pp 1919-1923, 2000.
[6] P. Nguyen, H. TNg, TYamada, M. K. Smith, J. Li, J. Han, M. Meyyappan, Nano Lett, pp 651-657, 2004.
[7] J. Cui, A. Wang, N. L. Edleman, J. Ni, P. Lee, N. R. Armstrong, T. J. Marks, Adv Mater, pp 1476-1480, 200.
[8] H. Zhu, X. Wang, F. Yang, X. Yang, Cryst. Growth & Des, pp 950-956, 2008.
[9] W. Schmid, N. Barsan, U. Weimar, Sensors and Actuators. B. Chemical. 3 (2003) 232-236.
[10] B. A. AKimov, A. V. Albul, A. M. Gaskov, V. Yu. Ilin, M. Labo, M. N. Rumyantseva, L. I. Ryabova, Phys. Tech. Semiconductors pp 400- 404, 1997.
[11] J. C. Manifacier, Thin Solid Films. 90 (1982) 297-308.
[12] W. R. Collin, Gustavo Serrano, Lindsay K. Wright, Hungwei Chang, Nicolás Nuñovero, and Edward T. Zellers, *Anal Chem*, pp 655–663, 2014.
[13] W. Gopel, Solid-state chemical sensors Sens. Actuators B. pp 167-193, (989.
[14] S. C. Leen, J. H. Lee, T. Sang, Y. H. Kim, Solar energy materials and solar cells, pp 481-487, 2003.
[15] E. Shanthi, Journal of Applied Physics. pp 6243-6251, 1980.
[16] G. Kienel, Thin Solid Films. pp 213-224, 1981.
[17] S. Muranaka, Y. Bando, T. Takada, Thin Solid Films, pp 11-13, 1981.
[18] C. A. Pan, T. P. Ma, Appl Phys Lett. pp 163–165, 1980.
[19] T. Tsung-Hsien; Y. Mu-Rong; W. She-Hung; C. Yi-Ping, J. solid state communication. pp 389-392, 2007.
[20] H. T. Yang, Y. T. Cheung, J. Cryst. Growth. pp 429-432, 1982.
[21] Rajiv K. Singh and J. Narayan, Physical Review B. pp 8843, 1990.
[22] M. Epifani, R. Díaz, J. Arbiol, P. Siciliano, and J. R. Morante, Chem. Mater. pp 840–846, 2006.
[23] L. Francioso, M. Russo, A. M. Taurino, P. Siciliano, Sensors and Actuators B: Chemical, pp 159–166, 2006.
[24] V. Musat, A. M. Rego, R. Monterio, E. Fortunato,. Microstructure and gas sensing properties of sol-gel ZnO thin films. Thin solid films, pp 1512-1515, 2008.
[25] G. Rangel-Porras, E. R. Ramirez, L. M. Torres-Guerra, J. of porous Materials, pp 69-78, 2010.
[26] A. B. Kashyout, M. Fathy, and M. B. Soliman,. Studying the Properties of RF-Sputtered Nanocrystalline Tin-Doped Indium Oxide, International Journal of Photoenergy, pp 6, 2011.
[27] Z. Qiao, R. Latz, and D. Mergel, Thin Solid Films, pp 250–258, 2004.
[28] F. Yakuphanoglu, S. Ilican, M. caglar, Y. caglar, J. optoelectronics and advanced materials, pp 2180-2185, 2007.
[29] http://refractiveindex. info/legacy/?group=CRYSTALS& material

Licensed Under Creative Commons Attribution CC BY